Brain Topogr
DOI 10.1007/s10548-016-0478-2

ORIGINAL PAPER

Independent Vector Analysis for SSVEP Signal Enhancement, Detection, and Topographical Mapping

Darren K. Emge[1] · François-Benoît Vialatte[2] · Gérard Dreyfus[2] · Tülay Adalı[1]

Received: 20 July 2015 / Accepted: 18 February 2016

Abstract Steady state visual evoked potentials (SSVEPs) have been identified as an effective solution for brain computer interface (BCI) systems as well as for neurocognitive investigations. SSVEPs can be observed in the scalp-based recordings of electroencephalogram signals, and are one component buried amongst the normal brain signals and complex noise. We present a novel method for enhancing and improving detection of SSVEPs by leveraging the rich joint blind source separation framework using independent vector analysis (IVA). IVA exploits the diversity within each dataset while preserving dependence across all the datasets. This approach is shown to enhance the detection of SSVEP signals across a range of frequencies and subjects for BCI systems. Furthermore, we show that IVA enables improved topographic mapping of the SSVEP propagation providing a promising new tool for neuroscience and neurocognitive research.

Keywords Independent vector analysis (IVA) · Steady state visual evoked potentials (SSVEP) · Brain computer interface (BCI)

This is one of several papers published together in Brain Topography on the "Special Issue:Multisubject decomposition of EEG - methods and applications".

✉ Darren K. Emge
demge1@umbc.edu

Tülay Adalı
adali@umbc.edu

[1] Department of Computer Science and Electrical Engineering, University of Maryland, Baltimore County, 1000 Hilltop Circle, Baltimore, MD 21250, USA

[2] SIGnal processing and MAchine learning (SIGMA) lab, ESPCI ParisTech, 10, rue Vauquelin, 75231 Paris Cedex 05, France

Introduction

Steady state visual evoked potentials (SSVEPs) are of interest in cognitive and clinical neuroscience, as well as neuro-engineering, making enhancement and detection of SSVEP signals an area of active research. The SSVEPs are evoked signals observed in electroencephalography (EEG), which are elicited when a subject observes a periodic visual stimulus, e.g., a reversing checkerboard. This elicited signal is a stable, long lived response that contains frequencies matching the visual stimulus as well as its harmonics (Vialatte et al. 2010). Although SSVEPs have a relatively stable spectrum, it is a low amplitude signal that is recorded as part of the overall EEG. The recorded EEG signal can be contaminated by the presence of artifacts arising from muscular activities, movement, as well as the presence of electrodermal, electrovascular, and respiratory signals, which further complicates the detection of SSVEPs.

The main goal in the detection of SSVEPs is for use in brain computer interface (BCI) systems. A BCI system allows for direct connection between a human and a computer through a non-muscular communication channel. This communication channel can allow persons with severe physical handicaps to interact with their environment, e.g.,control of devices such as wheel-chairs. Moving beyond medical applications, the BCI interface can be used to control systems under situations of high physical stress where manual control is not feasible. Other candidate signals for BCI systems include evoked response potentials and sensor motor responses, both of which require advanced training, and suffer from a lower information transfer rates (Vialatte et al. 2010). Therefore SSVEPs are a desirable way for BCI systems to function: thus,

Published online: 03 March 2016

developing an effective, robust, and accurate method for SSVEP detection is of great significance.

Since SSVEPs are stationary signals within the EEG, averaging can be used to reduce transient noise effects (Müller-Putz et al. 2005). Each epoch is Fourier transformed, and the resulting power spectra are then averaged. These averages are individually inspected for the presence of the SSVEP stimulus frequency. This method is known in the literature as power spectral density analysis (PSDA). PSDA suffers from sensitivities to biological noise and requires relatively long time recordings in order to estimate the frequency content with sufficient resolution (Zhang et al. 2014). Alternate to averaging, use of canonical correlation analysis (CCA) (Hotelling 1936) and more recently of multiset CCA (MCCA) (Kettenring 1971; Zhang et al. 2013, 2014) have both been introduced. These methods maximize the correlation between the recorded EEG channel or channels with a set of sine and cosine references at the target frequency. However, SSVEPs suffer from small shifts in frequency, and hence shifted versions of the sines and cosines must also be included in the set of references. Additionally, individual variations in the response time of the visual cortex to the stimulus onset requires that a range of latencies be introduced as well. As this dynamic range is expanded to address the variations, the size of the reference set increases exponentially, becoming intractable. In practice, only a limited number of references are normally used. However, this can lead to severe misalignments between the signal and the references, resulting in degradation in performance. The need to accurately and succinctly define a set of reference signals, based on shape and latency, is a highly active area of research on its own (Zhang et al. 2014).

More general work in the detection of oscillatory brain signals is presented in both Dähne et al. (2014) and Nikulin et al. (2011). Using a CCA type framework, Dähne et al. (2014) introduces canonical source power correlation analysis (cSPoC) to find and estimate highly correlated signal envelopes of oscillatory sources. These estimated envelopes can contain different underlying frequencies which are not guaranteed to be a frequency of interest. Moreover cPSoC is based upon a non-convex optimization problem and as demonstrated, requires multiple restarts in order for the algorithm to determine the optimal solution (Dähne et al. 2014). The spatio-spectral decomposition (SSD) is another general oscillatory detection method introduced in Nikulin et al. (2011). The SSD utilizes a matrix version of a signal-to-noise-like ratio to enhance the presence of a known target signal. The SSD assumes a limited spectral range, on the order of a few Hertz, and that the noise is both smooth and monotonic. For the direct detection of a few known SSVEP target frequencies with limited frequency jitter the SSD method could prove useful.

In this work, we use the rich framework of joint blind source separation (JBSS) to take advantage of the multiple types of diversity present, second and higher order statistics as well as dependence across channels, in the EEG data to provide a robust method for SSVEP detection enhancement. Independent vector analysis (IVA) generalizes independent component analysis (ICA)—which has proven very useful for the analysis of medical imaging data—to multiple datasets and allows for use of multiple types of diversity, i.e., statistical properties (Adalı et al. 2014). In our application, we define each dataset as the group of epochs from a single EEG electrode to enable an effective use of diversity across multiple datasets. Thus, with the implementation we introduce, IVA can effectively enhance the SSVEP detection by making full use of the stationary nature of the SSVEP without the need to address variations in subject stimulus onset. We show the gains in performance using our IVA-based method and that it also promises new insights for neuroscience research through improved topography maps.

This paper is organized as follows. "Approach and Motivation" section provides a description of IVA and the motivation behind its application to this problem, along with a description of standard processing, PSDA. The data is then described and the metric to be utilized to compare IVA to PSDA is given. "Experimental Results" section demonstrates the stability of IVA, its performance enhancement and looks at SSVEP propagation through topographic analysis. In "Discussion" section, we discuss our findings in detail.

Approach and Motivation

Independent Vector Analysis

Since the SSVEP is distributed across multiple EEG electrodes and propagates across the brain, a method that leverages the diversity across multiple datasets is highly desirable. IVA has been shown to be capable of using diversity within the data to estimate the underlying sources while exploiting diversity across all datasets in bio-medical applications such as in the analysis of multi-subject functional magnetic resonance imaging data (Adalı et al. 2014). In Emge et al. (2015), using three electrodes, we showed the promise of IVA to enhance the SSVEP content. In this paper, we introduce a complete IVA-based framework using epochs to define individual datasets from multiple electrodes and show how IVA can both significantly enhance the SSVEP content and reveal the topological

structure demonstrating the propagation of the SSVEP across the brain.

In our implementation, an EEG electrode recording or channel is broken into series of short time epochs, as shown in Fig. 1 on the left side. These groups of epochs across each EEG channel are treated as individual datasets. In this framework, we represent each epoch as a random vector using superscript notation as $\mathbf{x}^{[k]} = \left[x_1^{[k]}, \ldots, x_n^{[k]}, \ldots, x_N^{[k]}\right]^T$, with $k = 1, \ldots, K$, where K is the number of datasets (EEG channels), and N is the number of epochs for that channel. Assuming that each dataset is a linear mixture of N statistically independent sources, we can then use the generative mixture model, written as

$$\mathbf{x}^{[k]} = \mathbf{A}^{[k]}\mathbf{s}^{[k]} \quad k = 1, \ldots, K, \tag{1}$$

where each $\mathbf{A}^{[k]}$ is an N by N mixing matrix, containing the mixing profiles, and $\mathbf{s}^{[k]} = \left[s_1^{[k]}, \ldots, s_n^{[k]}, \ldots, s_N^{[k]}\right]^T$ is a random vector representing the signal sources for the kth dataset.

IVA simultaneously estimates the de-mixing matrices $\mathbf{W}^{[k]}$ for each dataset (epoch-broken EEG channel), which results in the source estimates

$$\mathbf{y}^{[k]} = \mathbf{W}^{[k]}\mathbf{x}^{[k]} \quad k = 1, \ldots, K, \tag{2}$$

where $\mathbf{y}^{[k]} = \left[y_1^{[k]}, \ldots, y_n^{[k]}, \ldots, y_N^{[k]}\right]^T$ is a random vector representing the source estimates for the kth dataset. The corresponding source estimates from each dataset, one from each, can be formed into a source component vector (SCV) written as $\mathbf{y}_n = \left[y_n^{[1]}, \ldots, y_n^{[k]}, \ldots, y_n^{[K]}\right]^T$, $n = 1, \ldots, N$. This is represented graphically in the right side of Fig. 1, where $F_{\mathbf{y}^{[k]}}(f)$ denotes the power spectra of the estimated sources for dataset k, and $F_{\mathbf{y}_n}(f)$ denotes the power spectral density of each SCV.

The IVA cost can then be written as

$$\mathcal{I}_{IVA}(\mathcal{W}) = \sum_{n=1}^{N}\left(\sum_{k=1}^{K}\mathcal{H}(y_n^{[k]}) - \mathcal{I}(\mathbf{y}_n)\right) - \sum_{k=1}^{K}\log\left|\det\mathbf{W}^{[k]}\right| - C \tag{3}$$

where $\mathcal{W}$ is the set of all de-mixing matrices, $\mathbf{W}^{[k]}$ are the individual demixing matrices to be estimated, $\mathcal{H}$ is the entropy of the source estimates, $\mathcal{I}$ is the mutual information within an SCV, and C is a constant. IVA thus minimizes the mutual information among the SCVs, while maximizing the entropy of the individual source estimates, as shown in (3). Thus IVA takes all the datasets into account simultaneously and maximizes dependence across the datasets (EEG channels) to enhance the SSVEP detection with the implementation we introduce.

The multivariate generalized Gaussian distribution (MGGD) is used to model the SCV density. The MGGD has a simple parametric form that is sufficiently flexible for most applications (Boukouvalas et al. 2015; Adalı et al. 2014; Anderson et al. 2013, 2012). All the marginals of the MGGD are generalized Gaussian distributed, a unimodal distribution which is is defined only by a scatter matrix and the shape parameter, β. The GGD can approximate distributions ranging from super-Gaussian (for $0 < \beta < 1$), Gaussian ($\beta = 1$), and to sub-Gaussian (for $\beta > 1$). This

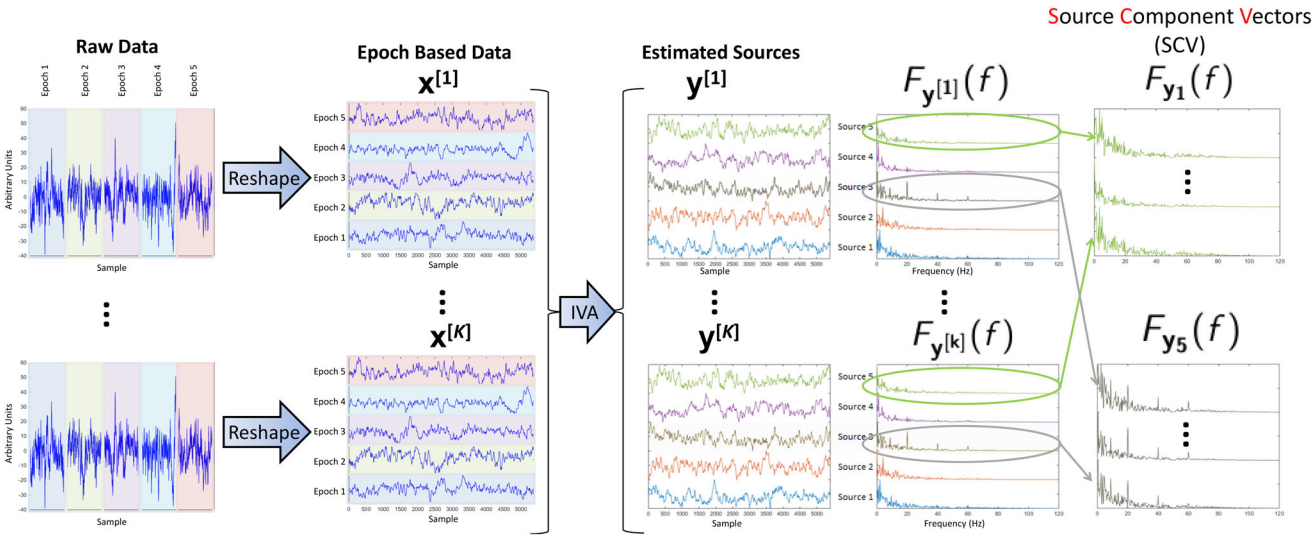

Fig. 1 The recorded EEG signals, shown on the *left half* of the diagram, are reshaped by breaking them into 5 3 second epochs, $\mathbf{x}^{[k]}$. The data is then processed using IVA and the resulting sources, $\mathbf{y}^{[k]}$, are estimated, which are then Fourier transformed, $\mathbf{F}_{\mathbf{y}^{[k]}}(f)$. The *right column* in the figure shows the PSD of SCVs, $\mathbf{F}_{\mathbf{y}_n}(f)$, and how IVA exploits the dependence across data sets (Color figure online)

implementation of IVA is known as IVA-GGD (Adalı et al. 2014; Anderson et al. 2013).

If we use a Gaussian distribution to model the SCV and constrain the demixing matrices to be orthogonal, then (3) becomes the IVA-G cost (Adalı et al. 2014; Anderson et al. 2012), which is equivalent to generalized variance (GENVAR) cost function proposed for achieving MCCA (Kettenring 1971). In fact, the IVA-GGD used in this work, is initialized using IVA-G. This initialization makes our starting point equivalent to MCCA, which we then utilize higher order statistics through the use of the MGGD model and the maximization of mutual information within the SCVs to improve the performance.

PSDA

The most widely used technique for the detection of SSVEP signals is power spectral density analysis. PSDA is applied separately to each EEG channel by breaking the recorded signal into short time epochs, on the order of a few seconds. The Fourier transform of each epoch is then computed, and the resulting power spectra are averaged to reduce the effects of transient noise and artifacts while enhancing the stationary SSVEP content. These averages are then analyzed to determine SSVEP content by looking for frequencies that match the stimuli.

Data

Participants consisted of eight healthy subjects having normal or corrected to normal vision with no history of migraine, epilepsy or any other neurological disorder. The experimental protocol was explained to all the participants before the experiment. The experiment followed the ethical guidelines of the Helsinki declaration (World Medical Association 2013), and all subjects filled out a consent form. Each subject performed three repetitions of the experiment, resulting in 24 total trials. Each trial consisted in observing a reversing checkerboard pattern at a single frequency for 15 seconds while 16 channels of EEG data were recorded, at 1.8 kHz, based upon the 10–20 international system (Klem et al. 1999). All electrodes were referenced to the FCz electrode, and the ground was located at AFz. Data were processed using a 50 Hz notch filter to remove power line noise and band pass filtered, with a pass band from 0.5 to 80 Hz.

In general, results presented in the literature cover the range from 6 to 21 Hz for SSVEP applications. To explore the full range of SSVEP and possible cognitive functions, four frequencies, 5, 10, 20, and 40 Hz, which include signals in the Theta (4–7 Hz), Alpha (8–15 Hz), Beta (16–31 Hz), and Gamma (> 32 Hz) ranges, are used in this work.

For both the PSDA and IVA methods, the 15 second data recordings for each channel are broken into five epochs. Each epoch is three seconds, a commonly used length (Parini et al. 2009), thus evenly dividing the data (left half of Fig. 1). The minimal data length is not investigated in this work. The division utilized for both methods allows for a direct comparison of the methods.

Performance Metric

Evaluation of the frequency content for PSDA averages and IVA source estimates is conducted using the signal-to-noise ratio at a given frequency, SNR_F introduced in Vialatte et al. (2010) and defined as

$$SNR_F = \frac{wF(f)}{\sum_{i=s}^{w/2} F(f + i\Delta f) + \sum_{i=s}^{w/2} F(f - i\Delta f)}, \quad (4)$$

where f is frequency, F is the energy of the signal at f, Δf is the frequency step size, and w is the window width. This metric estimates the signal-to-noise ratio at a given frequency using a symmetrical window about that frequency to estimate the noise value.

The SNR_F is applied to the PSDA and each of the source estimates from the IVA decomposition. In order to apply this method the ideal window width, w, is determined by varying the width and comparing the SNR_F for each width. The SNR_F dropped significantly due to the inclusion of a spike introduced by the next harmonic of the visual stimuli. Therefore, the window width is defined as approximately 1 Hz (three samples) less than the next harmonic of the target SSVEP stimulus.

Experimental Results

Stability of IVA

It is known that ICA algorithms that are of iterative nature suffer from stability issues (Du et al. 2014; Ma et al. 2011). To address the stability issues in ICA, one approach is to make use of the ICASSO (Himberg and Hyvärinen 2003) Matlab toolbox (Ma et al. 2011). In ICASSO, the algorithm is run multiple times, and the estimated components are clustered based upon a metric of similarity such as correlation, and then the best run is selected based upon the cluster centrotype. Since ICA also suffers from a permutation ambiguity, source estimates between runs can be inconsistent and the order can be variable between runs. Therefore, we must align the sources from the different runs using a method that can best sort and re-order the estimated components across multiple runs.

The IVA algorithms we use are also of iterative type and hence they suffer from the same stability and permutation ambiguity. Since IVA is an extension of ICA to multiple datasets, we use a similar approach to those used in ICA and run the IVA algorithm multiple times (runs) to determine the result that represents a consistent, i.e., stable, estimate for use as the final output. Since IVA was repeated for 10 runs, the maximum sum of the cross correlations (SCC) value is 10, and the most stable run is the run with the maximum SCC across the estimated sources for all datasets, i.e., closest to 10.

Since each run has a unique permutation ambiguity due to local optimal points in the cost function, we must first align the source estimates between runs. For our application to EEG time courses, alignment based on simple correlation of the estimated sources is used. Only one channel or dataset needs to be aligned for the IVA decomposition, since the permutation ambiguity within a single IVA run is shared by all datasets due to the maximization of the mutual information within each SCV, see (3). In this case, we choose the zero occipital channel, Oz, since the SSVEP is a visual evoked response which will be most prevalent in the occipital cortex. Once the sources are aligned, we calculate the SCC for each run and select the maximum. In general, the SCC values are similar across the runs, as shown in Table 1 for Subject 1, Experiment 1. In this example the most stable run is identified as run 1 (bold), which is used in all comparisons to demonstrate performance enhancement and topographic map generation.

Performance Enhancement

IVA exploits the diversity across data sets, in this case the epochs of 16 EEG channels, as well as the diversity within datasets, to estimate the underlying source components. In order to quantify the enhancement achieved by IVA over PSDA, the SNR_F values of the two methods are compared for the occipital zero channel, Oz. The Oz electrode is roughly located at the center of the visual cortex and since the SSVEP is a response to a visual stimulus, the strongest signals should be in this region, making it ideal for a direct performance comparison of the two methods. Examining the average of the differences across the 24 trials, Table 2 shows a consistent improvement to the SNR_F for IVA over PSDA. Statistical significance of these differences is established using a two-sample t test between the two sets of SNR_F scores. The t score, standard deviation (STD) and associate p values are listed in Table 2. All t scores are >3, implying that the difference is significant. This is confirmed by the low p values quantifying that IVA significantly improves the ability to detect the SSVEP.

Topographic Results

The enhanced detection of the SSVEP is essential for BCI systems, however by extending the analysis to include the propagation of the SSVEP across the brain reveals the possibility of additional applications in neuroscience research. Fig. 2 shows a comparison of the topography of the SSVEP for resting eyes open (REO) trial, no visual stimuli, and a trial with a 5 Hz flashing checkerboard. In Fig 2a, the topography shows the presence of a slight response in the areas near the visual cortex. Since the subject's eyes are open in this trial, the presence of energy, i.e., SNR_F in the posterior regions is not overly surprising. In fact, the analysis of the REO data for any SNR_F content revealed exponentially decreasing values, a trend that disappears around 40 Hz; this behavior is nearly identical for both PSDA and IVA. In Fig. 2b and c the SNR_F scores at 5 Hz for PSDA and IVA are shown for comparison. In Fig. 2b the topography resulting from PSDA shows elevated values in the posterior regions of the brain, central, parietal and occipital electrode locations. In Fig. 2c the IVA topology shows significant enhancement in the occipital electrode locations and across the topology in general. Looking closely at the central electrodes there is left side dominance in the calculated SNR_F scores which is also present upon closer examination of the frontal electrode F3 and F4 for the IVA topology. In Fig. 2b the PSDA topography shows a decrease in the frontal and pre-frontal response. This decrease can be explained by the sensitivity of PSDA to biological noise. SSVEPs occur in a large-scale functional occipitofrontal cortical network (Vialatte et al. 2010; Srinivasan et al. 2006, 2007; Pastor et al. 2007), therefore observing these frontal activations is of interest. IVA enhances the topography of these frontal networks as compared to PSDA.

Table 1 Example sum of cross correlation (SCC) values for Subject 1, Experiment 1

Run	1	2	3	4	5	6	7	8	9	10
SCC	**9.81**	9.64	*8.86*	9.71	9.77	9.70	9.74	9.80	9.71	9.79

For this subject the analysis was very stable, i.e., all SCC values are close to the maximum value of 10, with only one run, number 3 (italic), having a decreased value. The most stable run is selected based on the maximum SCC, in this case run 1 (bold)

Table 2 Enhancement averages for each SSVEP stimulus frequency, Avg Diff = $\mathrm{SNR}_F(IVA) - \mathrm{SNR}_F(PSDA)$. Two sample t test scores, sample standard deviation (STD), and associated p values for the two populations of SNR_F scores

Stimuli (Hz)	5	10	15	20	40
Avg diff	1.54	2.47	2.64	2.15	3.61
t score	3.81	4.18	3.97	3.44	3.30
STD	1.40	2.05	2.31	2.17	3.78
p value	4.16×10^{-4}	1.30×10^{-4}	2.52×10^{-4}	0.0012	0.0019

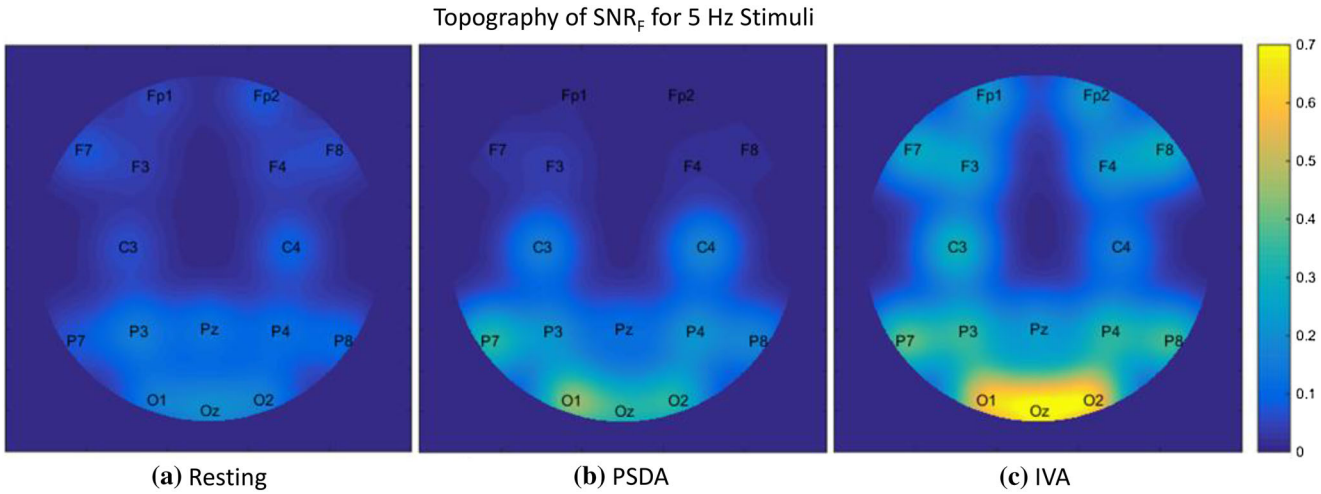

Fig. 2 SNR_F scores at 5 Hz for subject 001, experiment 1, run 1 for both **b** PSDA and **c** IVA. Data for resting state, no SSVEP signal present is presented in **a** for reference (Color figure online)

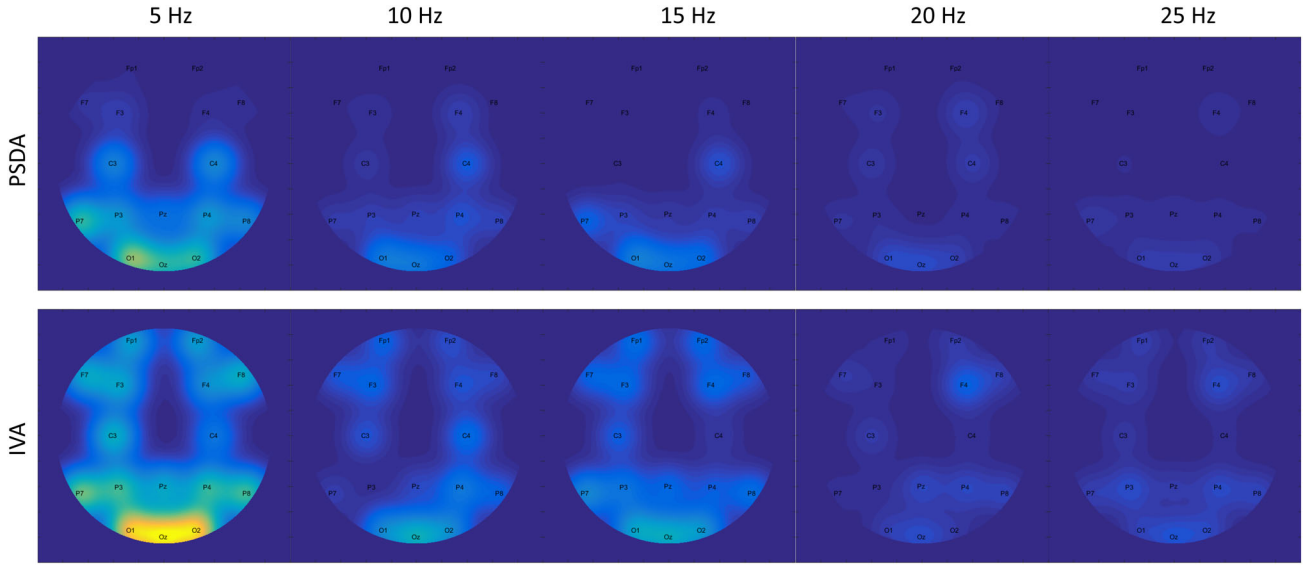

Fig. 3 SNR_F scores for Subject 1, Experiment 1, Run 1, with 5 Hz SSVEP. Topographic maps for the first five harmonics of the SSVEP target. The *top row* is for PSDA and the *bottom* is for IVA analysis (Color figure online)

Since the visual stimulus also elicits a response at the harmonics of the stimulus frequency, examination of the SSVEP propagation in those harmonics is presented in Fig. 3 for a 5 Hz stimulus frequency. Each row contains the fundamental frequency, $H_1 = 5$ Hz, and the first four harmonics, $H_2 = 10$, $H_3 = 15$, $H_4 = 20$, and $H_5 = 25$ Hz. In

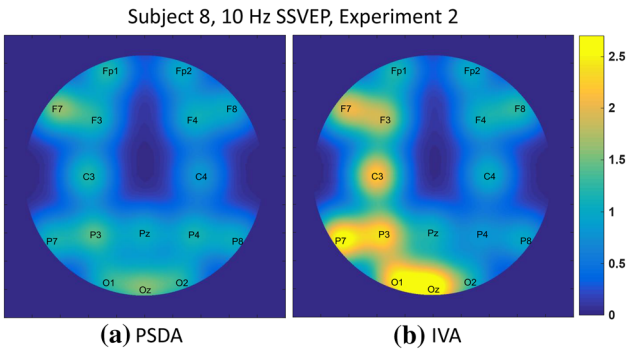

Fig. 4 SNR_F scores for Subject 8, Experiment 2, showing uni-lateral activation in the *left* hemisphere. The PSDA analysis **a** weakly shows *left* hemisphere dominance, whereas, the IVA analysis **b** shows significantly stronger left hemisphere activation

the upper row of topographies, the SSVEP propagation detected by PSDA is shown. The topography of the fundamental frequency reveals SSVEP content in the anterior regions of the brain. Harmonics H_1 and H_2, at 10 and 15 Hz respectively, show only a small SSVEP content in the visual cortex where the SSVEP is known to be strongest. There is some evidence of right hemisphere dominance in the C4 electrode site. The higher harmonics, in this case, show no SSVEP content.

The lower row of topographies are the SSVEP propagation revealed with IVA. As shown above, at the fundamental frequency, $H_1 = 5$ Hz, the topography revealed by IVA is enhanced across the entire brain, with some minor dominance found in the left hemisphere. As we move up through the harmonics, the SSVEP content continues to be present in different brain areas across the entire topography. There is a switch in lateral dominance for harmonics H_2 and H_3. The topographies for H_3 and H_4 show only minor SSVEP content, with the exception of F4, right side, for H_3.

Uni-lateral Effects

It has been shown that when a subject concentrates on a specific SSVEP stimuli, even in the presence of other SSVEP stimuli at different frequencies, that a uni-lateral response is indicative of the subject focusing on that particular stimuli, Kashiwase et al. 2012 and Kim et al. 2007. In the proposed IVA method, uni-lateral responses have been observed in several subjects and an example is shown in Fig. 4. For this subject, only a very minor uni-lateral response can be seen in the PSDA analysis, left side of Fig. 4. However, the IVA results show a significant activation in the left hemisphere for this subject up through the frontal areas, F7 and F3. This improved precision could be used to investigate the effects of ophtalmic conditions on SSVEP responses. For instance, it has been shown that SSVEP can be used as a marker for visual deficits (John et al. 2004) and asthenopia (Riddell et al. 2006).

Discussion

IVA has been shown to enhance the SSVEP detection by exploiting the diversity both within and across datasets as shown in Table 2. Statistical significance is established using a two-sample *t*-test across a range of frequencies and subjects. SSVEP propagation detected by IVA reveals enhancements for IVA over PSDA, not only at the fundamental frequency but in the first three harmonics as well. Closer examination of SSVEP propagation topographies reveals enhancements across the brain as well as changes in hemispheric dominance as a function of the harmonic.

The investigation of scalp topography based on the estimated sources containing SSVEP would be a promising tool in enhancing topographical probes, by providing insights into the SSVEP propagation mechanisms. The Gamma range (above 32 Hz) is of great interest as well for the investigation of cognitive mechanisms (Varela et al. 2001) and can be used to tag brain response topographies as they relate to visual tasks (Silberstein 1995). These potentials are shown to be useful in monitoring neural correlates of cognitive functions: for instance attention (Kim et al. 2006) or executive functions (Silberstein et al. 2003). However, the poor signal-to-noise ratio in higher EEG frequency ranges has made results obtained at frequencies above 25 Hz questionable. We have shown that IVA can extend the limits of EEG investigation, allowing for topographic probe investigations of cognitive mechanisms.

References

Adalı T, Anderson M, Fu G (2014) Diversity in independent component and vector analyses: identifiability, algorithms, and applications in medical imaging. IEEE Signal Process Mag 31(3):18–33

Anderson M, Adalı T, Li X (2012) Joint blind source separation with multivariate Gaussian model: algorithms and performance analysis. IEEE Trans Signal Process 60(4):1672–1683

Anderson M, Fu GS, Phlypo R, Adalı T (2013) Independent vector analysis, the Kotz distribution, and performance bounds. In: IEEE international conference on acoustics, speech and signal processing (ICASSP), pp 3243–3247

Boukouvalas Z, Fu GS, Adalı T (2015) An efficient multivariate generalized Gaussian distribution estimator: application to IVA. In: 2015 IEEE 49th annual conference on information sciences and systems (CISS), pp 1–4

Dähne S, Nikulin VV, Ramírez D, Schreier PJ, Müller KR, Haufe S (2014) Finding brain oscillations with power dependencies in neuroimaging data. NeuroImage 96:334–348

Du W, Ma S, Fu GS, Calhoun VD, Adalı T (2014) A novel approach for assessing reliability of ICA for FMRI analysis. In: IEEE international conference on acoustics, speech and signal processing (ICASSP), pp 2084–2088

Emge DK, Vialatte FB, Dreyfus G, Adalı T (2015) Independent vector analysis for SSVEP signal enhancement. In: 2015 IEEE 49th annual conference on information sciences and systems (CISS), pp 1–6

Himberg J, Hyvärinen A (2003) ICASSO: Software for investigating the reliability of ICA estimates by clustering and visualization. In: IEEE 13th workshop on neural networks for signal processing. NNSP'03., pp 259–268

Hotelling H (1936) Relations between two sets of variates. Biometrika 28:321–377

John FM, Bromham NR, Woodhouse JM, Candy TR (2004) Spatial vision deficits in infants and children with down syndrome. Investig Ophthalmol Vis Sci 45(5):1566–1572

Kashiwase Y, Matsumiya K, Kuriki I, Shioiri S (2012) Time courses of attentional modulation in neural amplification and synchronization measured with steady-state visual-evoked potentials. J Cogn Neurosci 24(8):1779–1793

Kettenring JR (1971) Canonical analysis of several sets of variables. Biometrika 58(3):433–451

Kim D, Wylie G, Pasternak R, Butler PD, Javitt DC (2006) Magnocellular contributions to impaired motion processing in schizophrenia. Schizophr Res 82(1):1–8

Kim YJ, Grabowecky M, Paller KA, Muthu K, Suzuki S (2007) Attention induces synchronization-based response gain in steady-state visual evoked potentials. Nat Neurosci 10(1):117–125

Klem GH, Lüders HO, Jasper H, Elger C (1999) The ten-twenty electrode system of the international federation. Electroencephalogr Clin Neurophysiol 52:3

Ma S, Correa NM, Li XL, Eichele T, Calhoun VD, Adalı T (2011) Automatic identification of functional clusters in fMRI data using spatial dependence. IEEE Trans Biomed Eng 58(12):3406–3417

Müller-Putz GR, Scherer R, Brauneis C, Pfurtscheller G (2005) Steady-state visual evoked potential (SSVEP)-based communication: impact of harmonic frequency components. J Neural Eng 2(4):123

Nikulin VV, Nolte G, Curio G (2011) A novel method for reliable and fast extraction of neuronal eeg/meg oscillations on the basis of spatio-spectral decomposition. NeuroImage 55(4):1528–1535

Parini S, Maggi L, Turconi AC, Andreoni G (2009) A robust and self-paced BCI system based on a four class SSVEP paradigm: algorithms and protocols for a high-transfer-rate direct brain communication. Comput Intell Neurosci. doi:10.1155/2009/864564

Pastor MA, Valencia M, Artieda J, Alegre M, Masdeu J (2007) Topography of cortical activation differs for fundamental and harmonic frequencies of the steady-state visual-evoked responses. An EEG and PET H215O study. Cereb Cortex 17(8):1899–1905

Riddell PM, Wilkins A, Hainline L (2006) The effect of colored lenses on the visual evoked response in children with visual stress. Optom Vis Sci 83(5):299–305

Silberstein RB (1995) Steady state visually evoked potentials, brain resonances and cognitive processes. Oxford University Press, New York

Silberstein RB, Danieli F, Nunez PL (2003) Fronto-parietal evoked potential synchronization is increased during mental rotation. NeuroReport 14(1):67–71

Srinivasan R, Bibi FA, Nunez PL (2006) Steady-state visual evoked potentials: Distributed local sources and wave-like dynamics are sensitive to flicker frequency. Brain topogr 18(3):167–187

Srinivasan R, Fornari E, Knyazeva MG, Meuli R, Maeder P (2007) FMRI responses in medial frontal cortex that depend on the temporal frequency of visual input. Exp Brain Res 180(4):677–691

Varela F, Lachaux JP, Rodriguez E, Martinerie J (2001) The brainweb: phase synchronization and large-scale integration. Nat Rev Neurosci 2(4):229–239

Vialatte FB, Maurice M, Dauwels J, Cichocki A (2010) Steady-state visually evoked potentials: focus on essential paradigms and future perspectives. Prog Neurobiol 90(4):418–438

World Medical Association (2013) World medical association declaration of helsinki: ethical principles for medical research involving human subjects. JAMA 310(20):2191

Zhang Y, Zhou G, Jin J, Wang M, Wang X, Cichocki A (2013) L1-regularized multiway canonical correlation analysis for SSVEP-based BCI. IEEE Trans Neural Syst Rehabil Eng 21(6):887–896

Zhang Y, Zhou G, Jin J, Wang M, Cichocki A (2014) L1-Regularization multiway cannonical correlation analysis for SSVEP-Based BCI. IEEE Trans Neural Syst Rehabil Eng 21(6):887–896